



# HHS Public Access

Author manuscript

*Ophthalmic Surg Lasers Imaging Retina*. Author manuscript; available in PMC 2016 January 14.

Published in final edited form as:

*Ophthalmic Surg Lasers Imaging Retina*. 2014 ; 45(6): 614–617. doi:10.3928/23258160-20141118-20.

## High-Speed Ultrahigh-Resolution OCT of Bruch's Membrane in Membranoproliferative Glomerulonephritis Type 2

**Mehreen Adhi, MD, Sarah P. Read, MD, PhD, Jonathan J. Liu, PhD, James G. Fujimoto, PhD, and Jay S. Duker, MD**

New England Eye Center, Tufts Medical Center, Boston, Massachusetts (MA, SPR, JSD); and Department of Electrical Engineering and Computer Science, Research Laboratory of Electronics, Massachusetts Institute of Technology, Cambridge, Massachusetts (JLL, JGF)

### Abstract

Membranoproliferative glomerulonephritis (MPGN) type 2 is characterized by electron-dense deposits in the glomerular basement membrane and drusen-like deposits in Bruch's membrane. Over time, atrophic changes in the retina and retinal pigment epithelium occur, which can progress to choroidal neovascularization (CNV). This report describes a patient with MPGN type 2 who developed progressive loss of vision secondary to CNV. High-speed ultrahigh-resolution optical coherence tomography (UHR-OCT) showed an irregular Bruch's membrane that measured 10  $\mu\text{m}$  beneath the foveal center. High-speed UHR-OCT can potentially be used to analyze Bruch's membrane in secondary ocular manifestations of diseases such as MPGN type 2 and primary retinal diseases such as age-related macular degeneration.

### INTRODUCTION

Membranoproliferative glomerulonephritis type 2 is a complex genetic disease that typically presents in children between the ages of 5 and 15 years and leads to end-stage renal disease.<sup>1</sup> Ocular manifestations of membranoproliferative glomerulonephritis (MPGN) type 2 include drusen-like deposits in Bruch's membrane.<sup>2</sup> The composition of these deposits is similar to that of drusen in age-related macular degeneration (AMD), consistent with the current understanding that both share a complement-mediated pathogenesis.<sup>3</sup> Over time, atrophic changes in the retina and retinal pigment epithelium (RPE) become manifest and can eventually progress to choroidal neovascularization (CNV).<sup>1</sup>

This report describes a patient with end-stage renal disease due to MPGN type 2 who presented with CNV in his left eye. High-speed ultrahigh-resolution optical coherence tomography (UHR-OCT) findings are described.

Address correspondence to Jay S. Duker, MD, New England Eye Center, 800 Washington Street, Boston, MA 02111; 617-636-4677; fax: 617-636-4866; [jduker@tuftsmedicalcenter.org](mailto:jduker@tuftsmedicalcenter.org).

Dr. Fujimoto receives royalties from intellectual property owned by MIT and licensed to Carl Zeiss Meditec and Optovue and has stock options in Optovue. Dr. Duker receives research support from Carl Zeiss Meditec and Optovue. The remaining authors have no financial or proprietary interest in the materials presented herein.

## CASE REPORT

A 29-year-old man was referred to the New England Eye Center at Tufts Medical Center in Boston in 1999 for further management of a submacular CNV in his right eye. He had been treated previously with focal laser. He had a history of hypertension and end-stage renal disease requiring hemodialysis due to MPGN type 2 that was confirmed on renal biopsy. Of note, he was allergic to sodium fluorescein.

On initial evaluation, his right eye had a best corrected visual acuity (BCVA) of 20/40 without active CNV. His left eye had a BCVA of 20/20 and RPE mottling or drusen-like deposits in the macula without evidence of CNV. Over the ensuing 18 months, he developed recurrent CNV in the right eye that was unresponsive to focal laser, photodynamic therapy, and intravitreal corticosteroid injections. His BCVA eventually deteriorated to no light perception in the right eye after massive subretinal hemorrhage. The left eye remained stable on regular yearly follow-up examination for 12 years. Figure 1 shows the color fundus photographs from 2003. In 2009, an OCT of the left eye using a prototype high-speed UHR-OCT system (an investigational OCT device approved by the institutional review boards of Tufts Medical Center and Massachusetts Institute of Technology) with an axial resolution of approximately 3  $\mu\text{m}$  in tissue was performed. This showed a detached RPE and an irregular Bruch's membrane that was seen as a prominent hyper-reflective line just below the level of the RPE (Figure 2). The width of the hyperreflective line was measured to be 10  $\mu\text{m}$  beneath the foveal center (Figure 2).

In 2012, 12 years after his initial visit, the patient presented with new distortion of vision in the left eye. His BCVA was 20/20, and dilated fundus examination showed new areas of hemorrhage and subretinal fluid superonasal to the macula (Figure 3, page 616). Indocyanine green angiography showed no definitive signs of CNV (Figure 3), but OCT imaging using the commercially available spectral-domain OCT (SD-OCT) (Cirrus; Carl Zeiss Meditec, Dublin, CA) showed subretinal hemorrhage and fluid nasally (Figure 3). He was treated with intravitreal bevacizumab (1.25 mg) and focal laser. Intravitreal bevacizumab was repeated every 6 weeks for the subsequent year. At his most recent follow-up visit in 2013, after nine intravitreal bevacizumab injections, BCVA was 20/25, with minimal persistent extrafoveal subretinal hemorrhage and fluid (Figure 4, page 617).

## DISCUSSION

This report describes a patient with end-stage renal disease due to MPGN type 2 who developed CNV, first in his right eye leading to complete loss of vision, and then many years later in his left eye that was successfully treated with intravitreal bevacizumab. Previous reports of patients with MPGN type 2 have reported retinal thinning and drusen-like RPE elevation using SD-OCT.<sup>4</sup> Novel high-speed UHR-OCT imaging in this patient suggests an irregular and prominent Bruch's membrane measuring 9 to 13  $\mu\text{m}$  at three locations.

Analysis of alterations in Bruch's membrane is an emerging area of interest due to such changes being associated with disease states such as AMD. On histology, Bruch's

membrane in the macular region of healthy eyes varies in thickness from 2 to 4.7  $\mu\text{m}$ .<sup>6</sup> Currently available commercial SD-OCT systems and the new swept-source OCT technology offer an axial resolution of 5 to 7  $\mu\text{m}$  in tissue and are therefore usually unable to delineate Bruch's membrane independent from the RPE in healthy eyes. In patients with detachment of RPE, Bruch's membrane is seen as a hyper-reflective line just below the level of the RPE.<sup>7</sup> In the present case, a prototype high-speed UHR-OCT with an axial resolution of approximately 3  $\mu\text{m}$  in tissue showed an irregular and prominent Bruch's membrane (Figure 2, page 615), a finding consistent with previous histopathological analysis in patients with MPGN type 2.<sup>2</sup> The measurements of the Bruch's membrane on high-speed UHR-OCT were comparable to those obtained on the commercially available SD-OCT, although the two OCT images were not consecutive in the present case.

Quantification of the thickness of Bruch's membrane using OCT is not a validated method owing to the limited resolution of the OCT systems currently in commercial and research use. As OCT technology advances, systems with high axial resolutions closer, if not comparable, to histology<sup>8</sup> may be helpful in detecting subtle early changes in diseases that exhibit a histologically proven thickening of Bruch's membrane such as AMD<sup>9</sup> and MPGN type 2.<sup>2</sup> In MPGN type 2 such as in this case, only invasive renal biopsy can predict the changes in glomerular basement membrane. An in vivo assessment using OCT in these patients could possibly predict the progression of renal disease with the caveat that an accurate assessment may be limited by the inherent resolution of the OCT system.

In conclusion, the present report is unique for two reasons. First, it describes a case of CNV secondary to MPGN type 2 imaged with a high-resolution OCT system. Second, the OCT images revealed an irregular and prominent Bruch's membrane consistent with the known histopathologic changes in this disease. It is expected that the improved axial resolution achieved by high-speed UHR-OCT may be able to reveal subtle Bruch's membrane changes in diseases such as MPGN type 2 and AMD.

## Acknowledgments

Supported in part by a Research to Prevent Blindness unrestricted grant to the New England Eye Center, NIH contracts R01-EY11289-27, R01-EY13178-12, R01-EY013516-09, and R01-EY018184-05, Air Force Office of Scientific Research FA9550-10-1-0551, FA9550-10-1-0063, and FA9550-12-1-0499, and the Massachusetts Lions Club.

## References

1. McAvoy CE, Silvestri G. Retinal changes associated with type 2 glomerulonephritis. *Eye*. 2005; 19(9):985–989. [PubMed: 15375355]
2. Duvall-Young J, MacDonald MK, McKechnie NM. Fundus changes in (type II) mesangiocapillary glomerulonephritis simulating drusen: a histopathological report. *Br J Ophthalmol*. 1989; 73(4): 297–302. [PubMed: 2713310]
3. D'Souza YB, Jones CJ, Short CD, Roberts IS, Bonshek RE. Oligosaccharide composition is similar in drusen and dense deposits in membranoproliferative glomerulonephritis type II. *Kidney Int*. 2009; 75(8):824–827. [PubMed: 19177159]
4. Ritter M, Bolz M, Haidinger M, et al. Functional and morphological macular abnormalities in membranoproliferative glomerulonephritis type II. *Br J Ophthalmol*. 2010; 94(8):1112–1114. [PubMed: 20679091]

5. The Southwest Pediatric Nephrology Study Group. Dense deposit disease in children: prognostic value of clinical and pathologic indicators. *Am J Kidney Dis.* 1985; 6(3):161–169. [PubMed: 3876030]
6. Ramrattan RS, van der Schaft TL, Mooy CM, de Bruijn WC, Mulder PG, de Jong PT. Morphometric analysis of Bruch's membrane, the choriocapillaris, and the choroid in aging. *Invest Ophthalmol Vis Sci.* 1994; 35(6):2857–2864. [PubMed: 8188481]
7. Yoshida M, Abe T, Kano T, Tamai M. Two types of optical coherence tomography images of retinal pigment epithelial detachments with different prognosis. *Br J Ophthalmol.* 2002; 86(7):737–739. [PubMed: 12084740]
8. Drexler W, Morgner U, Ghanta RK, Kartner FX, Schuman JS, Fujimoto JG. Ultra-high resolution optical coherence tomography. *Nat Med.* 2001; 7(4):502–507. [PubMed: 11283681]
9. Grindle CF, Marshall J. Ageing changes in Bruch's membrane and their functional implications. *Trans Ophthalmol Soc UK.* 1978; 98(1):172–175. [PubMed: 285503]

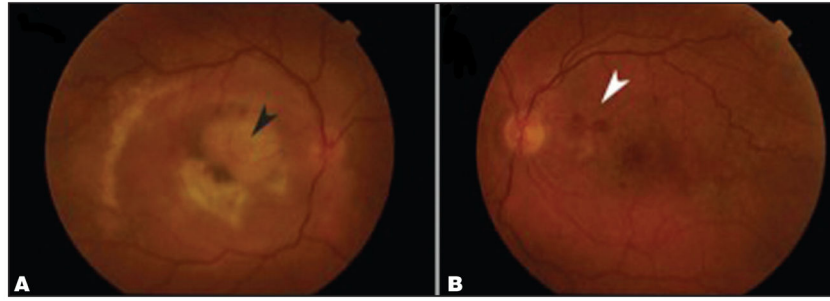


**Figure 1.** (A) Fundus photograph of the right eye shows a large disciform scar and scarring from prior subretinal hemorrhages and laser treatments (black arrow). (B) Fundus photograph of the left eye shows retinal pigment epithelium changes in the macula and extrafoveal hemorrhages (white arrow). Drusen-like deposits are visible throughout posterior pole.

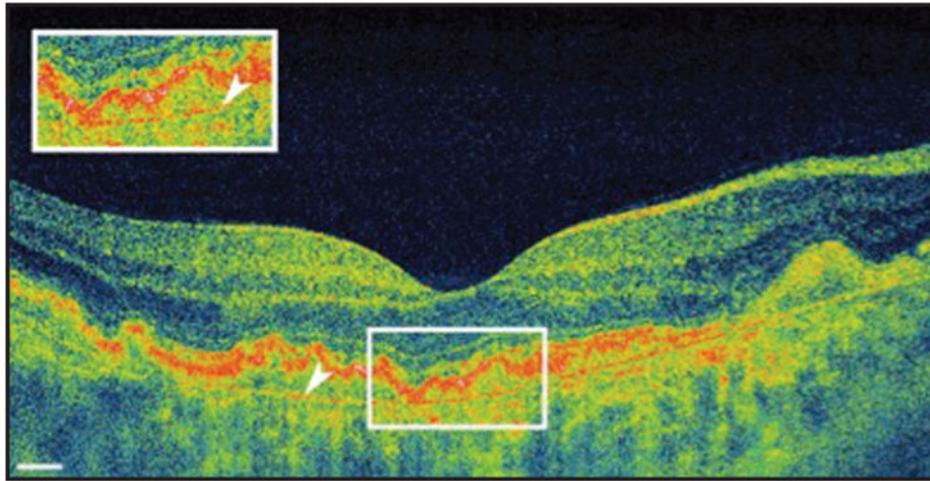


**Figure 2.** High-speed ultrahigh-resolution OCT image of the left eye shows detachment of the retinal pigment epithelium and an irregular and prominent Bruch's membrane seen as a hyperreflective line just below the level of the retinal pigment epithelium (white arrow) measuring 10  $\mu\text{m}$  beneath the fovea, 9  $\mu\text{m}$  at 1 mm temporal to the fovea, and 13  $\mu\text{m}$  at 1 mm nasal to the fovea. Scale bar = 300  $\mu\text{m}$ .

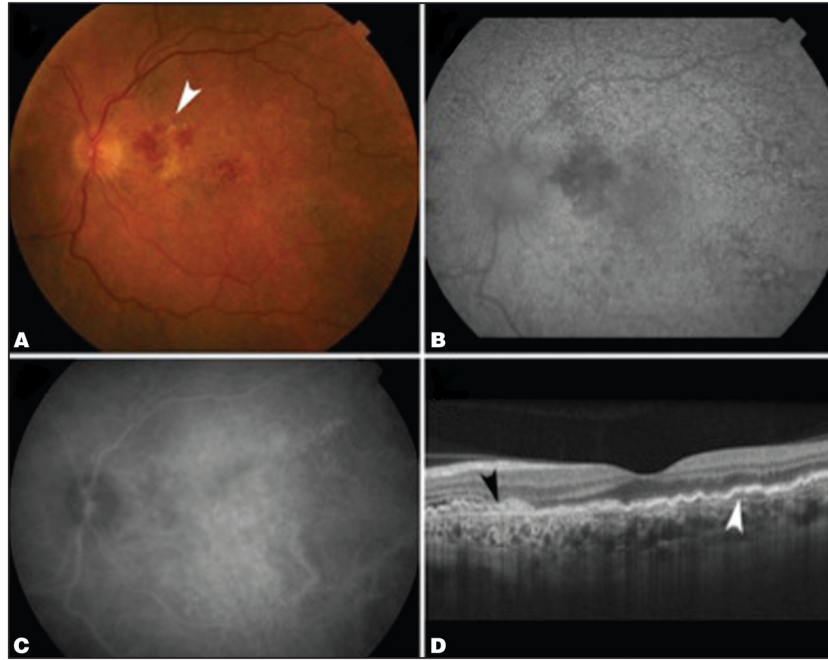


**Figure 3.**

(A) Fundus photograph of the left eye shows chronic retinal pigment epithelium changes with new areas of extrafoveal hemorrhage and fluid (white arrow). (B) Fundus autofluorescence of the left eye shows scattered drusen-like deposits. (C) Indocyanine green angiography of the left eye did not show any definitive choroidal neovascularization. (D) OCT of the left eye obtained using the commercially available spectral-domain system revealed subretinal fluid nasally, pigment epithelial detachments (white arrow), and features consistent with choroidal neovascularization (black arrow).

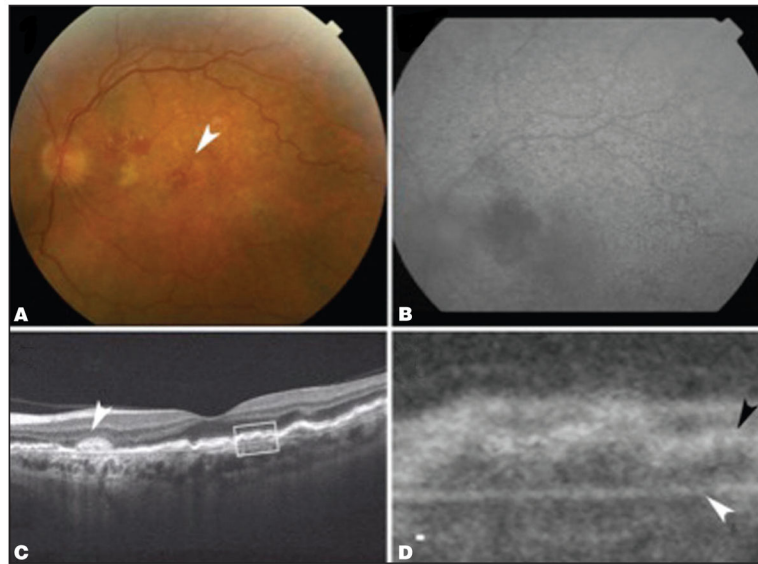


**Figure 4.**

(A) Fundus photograph of the left eye shows continued central pigmentary changes in the macula (white arrow), flat extrafoveal hemorrhage and fluid, and pigment and drusen-like deposits in the periphery. (B) Fundus autofluorescence of the left eye shows drusen-like deposits. (C) OCT image of the left eye using the commercially available spectral-domain system showed numerous drusen-like deposits and pigment epithelial detachments (white arrow) with no evidence of fluid. (D) Higher magnification of the OCT image shows a detached retinal pigment epithelium (RPE) and a prominent Bruch's membrane (white arrow) seen as a hyperreflective line just below the level of RPE that measured 9  $\mu\text{m}$  beneath the fovea, 8  $\mu\text{m}$  at 1 mm temporal to the fovea, and 12  $\mu\text{m}$  at 1 mm nasal to the fovea using the linear measurement tool available on the spectral-domain OCT system. The retinal pigment epithelium (black arrow) is detached from Bruch's membrane. Scale bar = 10  $\mu\text{m}$ .